RESEARCH ARTICLE

Assessing spatial and temporal patterns of canopy decline across a diverse montane landscape in the Klamath Mountains, CA, USA using a 30-year Landsat time series

Drew S. Bost ⬤ · Matthew J. Reilly · Erik S. Jules · Melissa H. DeSiervo · Zhiqiang Yang · Ramona J. Butz

Abstract

Context Tree mortality is of considerable concern, but the magnitude and extent of forest canopy decline are relatively unknown in landscapes with high levels of topographic complexity, spatial heterogeneity, and species diversity. We assessed 30 years of canopy decline, including a 5-year period characterized by extreme drought, in one of North America's most diverse landscapes in the Klamath Mountains of northern California, USA.

Objectives (1) Characterize tree mortality by species, (2) Quantify temporal and spatial patterns of remotely-sensed canopy decline in relation to climate, (3) Compare canopy decline among vegetation types, topographic settings, and stand structural classes during drought.

Methods We characterized tree mortality by species with field data and quantified the role of climate on canopy decline with a 30-year Landsat time series. We assessed and compared the role of topography and stand structure on canopy decline during drought.

Results Most tree mortality and canopy decline occurred at higher elevations in Shasta red fir (*Abies magnifica* var. *shastensis*) and subalpine forests. Annual area of canopy decline was positively correlated with summer temperature and minimum vapor pressure deficit but not precipitation. The area of canopy decline was three times greater during the drought. The magnitude of decline was greatest at higher elevations, on more exposed, southwestern slopes, and in stands with old-growth structure. Stands in valleys and low slopes experienced relatively little decline.

D. S. Bost (✉) · M. J. Reilly · E. S. Jules
Department of Biological Sciences, Humboldt State University, 1 Harpst Street, Arcata, CA 95521, USA
e-mail: db111@humboldt.edu

M. H. DeSiervo
Department of Biological Sciences, Dartmouth College, Hanover, NH 03755, USA

Z. Yang
USDA Forest Service, Rocky Mountain Research Station, 507 25th Street, Ogden, UT, USA

R. J. Butz
USDA Forest Service Pacific Southwest Region, 1330 Bayshore Way, Eureka, CA 95501, USA

R. J. Butz
Department of Forestry and Wildland Resources, Humboldt State University, 1 Harpst Street, Arcata, CA 95521, USA

Conclusions Our study demonstrates the vulnerability of high elevation, old-growth forests to increasing temperature and suggests the potential for refugia from drought in diverse, heterogeneous landscapes.

Introduction

Recent warming temperatures and reduced precipitation have produced longer and hotter droughts, leading to marked increases in tree mortality worldwide (Allen et al. 2010). Elevated background mortality rates and mortality events are occurring with increasing frequency (van Mantgem et al. 2009; Bentz et al. 2010; Reilly and Spies 2016; Hart et al. 2017; Bell et al. 2018), driven in part by drought stress which weakens trees' physiological defenses against pests and pathogens, making them more likely to die from infestation or infection (Manion 1991; Anderegg et al. 2012; Williams et al. 2013). Climate-induced mortality can cause large shifts in species composition as well as changes in ecosystem structure and function (Klos et al. 2009; van der Molen et al. 2011), but the magnitude and extent of forest decline events are relatively unknown in landscapes with high levels of topographic complexity, spatial heterogeneity, and species diversity (Allen et al. 2010).

Several regions experiencing widespread tree mortality events and canopy decline associated with climate change have garnered significant attention among researchers in North America (e.g., Guarín and Taylor 2005; van Mantgem and Stephenson 2007; Battles et al. 2008; Williams et al. 2013). Lodgepole pine (*Pinus contorta*) forests of Northern Colorado, Southern Wyoming and British Columbia have seen large outbreaks of mountain pine beetle (*Dendroctonus ponderosae*) associated with decreased winter snowpack and warmer winters (Williams and Liebhold 2002; Biederman et al. 2014). While studying these events has been important for our understanding of the climatic mechanisms driving tree mortality and canopy decline, these ecosystems are relatively homogeneous in terms of species composition and canopy dominance. Tree mortality may vary spatially in

landscapes with higher levels of topographic complexity, variable stand structure, and taxonomic diversity (Paz-Kagan et al. 2017), but relatively little is known on how mortality is related to local heterogeneity.

Remote sensing has proven to be a highly effective means to quantify and assess tree mortality and forest disturbance (Kennedy et al. 2012; Meddens et al. 2013; Cohen et al. 2016; Bell et al. 2018), especially in landscapes where it is difficult or expensive to conduct field-based studies. The use of remote sensing offers a unique perspective into the dynamics of forest disturbance and climatic drivers of ecosystem change by assessing the timing and spatial patterns of mortality on a broader scale than what field-measured data offers by itself. In particular, field-based studies are often limited in their ability to detect the timing and spatial patterns of mortality at broad spatial scales. The spatial and temporal resolution of Landsat imagery has proven to be effective for analyzing large-scale forest mortality and changes in forest cover over long periods of time (Kennedy et al. 2009). Landsat time series analysis, whereby annual, pixel-based change is detected through tracking spectral trajectories across a landscape, is frequently used to detect forest disturbance and canopy decline (Morawitz et al. 2006; Goodwin et al. 2008; Wulder et al. 2008; Vogelmann et al. 2009; Cohen et al. 2010; Meddens et al. 2012; Cohen et al. 2016; Potter 2016; Van Gunst et al. 2016).

The Klamath Mountains of northern California and southwestern Oregon are renowned for their high levels of taxonomic diversity and heterogenous mosaic of vegetation types (Whittaker 1960; Stebbins and Major 1965; Sawyer 2007). This remote region contains steep climatic gradients that give rise to exceptionally high endemism and plant species richness (Coleman and Kruckeberg 1999). Fire has historically been an important type of forest disturbance (Taylor and Skinner 2003), and much of the tree mortality-related research in this region has focused on the effects of wildfires on vegetation communities (Odion et al. 2004; Miller et al. 2009). Recent studies have started to document more subtle changes in vegetation associated with climate change (Copeland et al. 2016; DeSiervo et al. 2018).

The overall objective of this study was to quantify temporal and spatial patterns of forest decline in the Russian Wilderness using a Landsat time series

analysis. By coupling annualized Landsat images across 30 years (1986–2016) with field-based measurements, we quantified mortality and canopy decline in four forest types and assessed the contribution of different climatic and topographic variables on canopy decline. Specifically, the main objectives of this study were to (1) characterize tree mortality by species using field data, (2) quantify temporal and spatial patterns in the extent and magnitude of canopy decline with a 30-year Landsat time series, (3) assess the relationship between topographic and structural attributes with magnitude of canopy decline, and (4) assess the role of climate in regards to canopy decline. In the face of recent major droughts throughout California and around the world, understanding how forests may be impacted by projected changes in climate will be critical to anticipating how the structure and composition of forests may change in the future.

Methods

Study region

The study site was located in the Russian Wilderness, a 51 km^2 wilderness area in the east central portion of the Klamath Mountains in northern California (41°17′N, 122°57′W) (Fig. 1). The Russian Wilderness is a mountainous landscape ranging from 760 to 2500 m and is comprised of granodiorite parent material. This wilderness provides a unique study area for documenting changes in forest structure due in part to its high diversity of conifer species and vegetation types (Sawyer and Thornburgh 1974). There are 18 documented conifer species within the wilderness boundaries, representing one of the highest species richness of conifer taxa on record (Kauffmann 2012).

Common forest types range from lower elevation mixed conifer forest containing ponderosa pine (*Pinus ponderosa*), lodgepole pine, and Douglas-fir (*Pseudotsuga menziesii*); upper elevation mixed conifer forests containing white fir (*Abies concolor*), Shasta red fir (*Abies magnifica* var. *shastensis*), and western white pine (*Pinus monticola*); and subalpine forest types containing Shasta red fir, mountain hemlock (*Tsuga mertensiana*) and whitebark pine (*Pinus albicaulis*) (Sawyer and Thornburgh 1971, 1974). This botanical diversity was the primary reason that

portions of the wilderness were designated as Forest Service Management Areas, split between the southern Sugar Creek Research Natural Area (RNA) and the northern Duck Lake Botanical Area (Sawyer and Thornburgh 1971; Keeler-Wolf 1984).

Fire occurrence was historically most frequent at low elevations in mixed conifer and white fir forests with average fire return intervals ranging from 12 to 25 years (Wills and Stuart 1994; Taylor and Skinner 1998, 2003). There are fewer fire history studies in the region for the higher elevation forest types, but Skinner (2003) reports mean fire return intervals of < 30 years in upper montane and subalpine lake basins in the Klamath Mountains. Fire return intervals in red fir forests of the eastern Cascades range from a low of 16 to 42 years (Taylor and Halpern 1991; Taylor 1993), 9 to 100 years (Bekker and Taylor 2001, 2010) and 26 to 109 years (Taylor 2000) and also suggest an important role of low severity fire in this high elevation forest type of northern California. Prior to late summer of 2014, there is little evidence that this landscape had experienced a large wildfire in over 100 years. Although low- and mid-elevation vegetation types missed the most fire cycles, the relatively frequent historical fire regime of higher elevation forest types suggests that red fir and subalpine forests have also experienced the effects of fire exclusion (Safford and Van de Water 2014).

Field sampling

To characterize tree mortality, field plots were established in the summer of 2015 as part of a previous study documenting recent tree mortality in the Russian Wilderness (DeSiervo et al. 2018). The original 2015 dataset consisted of 144 fixed-radius plots with radii of 11.37 m (0.04 ha). Only plots that were within the four main forest types were included (see below), for a total of 116 plots (Table 1). Within each plot, information was recorded on species and status (live, unhealthy, and dead) for all trees ≥ 7.6 cm diameter at breast height (dbh). The designation of "unhealthy" was assigned to trees with substantial physical damage (either mechanically or biotically generated) and poor or very poor crown vigor. Standing dead trees were given a decay rating ranging from recent (1) to older (5) mortality based on the classification system of Cline et al. (1980). Snags assigned a decay rating of recent (1) typically had all branches remaining and
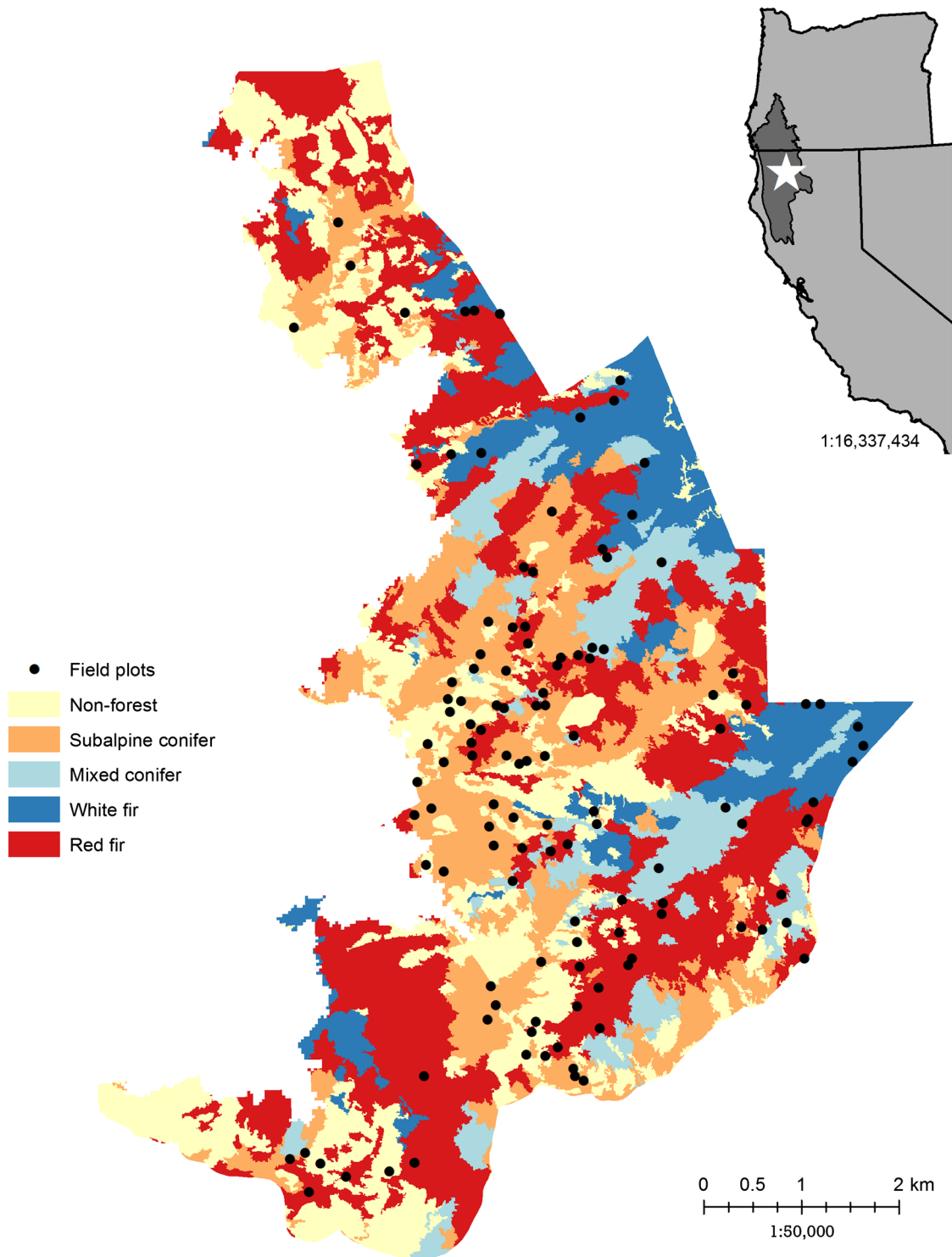
Fig. 1 Map of the study area in the Russian Wilderness, CA, located within the east-central extent of the Klamath Region (shown on locator map). Plot data was collected in summer of 2015. Forest type data is from the 2014 CALVEG dataset (Parker and Matyas 1979)

Table 1 Summary data on forest types for the Russian Wilderness, CA. Plots were taken in the summer of 2015

Forest type	# plots	Elevation (m)	Total area (ha)
Mixed conifer	12	1539–2326	419.9
White fir	23	1480–2243	652.5
Red fir	45	1561–2313	1856.3
Subalpine conifer	36	1703–2482	1001.0

most needles and bark present. Species with less than 60 individuals were removed from the dataset to ensure more accurate comparison between species. Tree measurements were summarized by live, unhealthy, and dead basal area (BA) in units of m^2 for each species and within each plot.

Remote sensing and spatial analysis

Because our study focused primarily on conifer tree mortality and disturbance, the study area was divided into dominant forest types using the Classification and Assessment with Landsat of Visible Ecological Groupings (CALVEG) system. CALVEG uses a combination of Landsat spectral signatures and field verification to determine vegetation types across the state of California (Parker and Matyas 1979). To simplify comparison among forest types, the original CALVEG classifications were reduced from nine to four dominant overstory groupings: subalpine conifer, red fir, mixed conifer, and white fir. The groupings were made by manually assessing CALVEG's original vegetation descriptions and combining forest types that had similar understory and overstory species composition and elevation ranges. For example, the subalpine conifer forest type is a combination of the subalpine conifer and mountain hemlock cover types. Combined categories were also compared to field-measured species composition and cover classes to ensure that new categories were accurately represented (Fig. 2).

Radiometrically corrected and georectified Landsat TM, ETM+ and OLI 8 images were selected within the growing season (June–August) between the years of 1986 and 2016. Images were processed using the LandTrendr algorithms which are described in detail in Kennedy et al. (2010). Briefly, Landsat images were selected and aggregated to create annual medoid
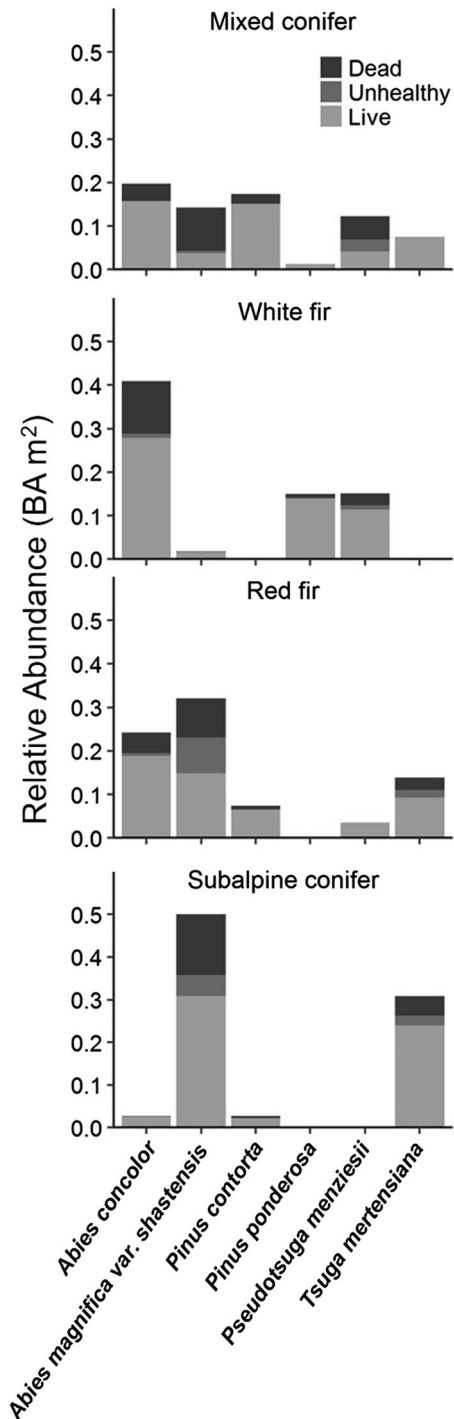
Fig. 2 Comparison of basal area (BA) among four forest types in the Russian Wilderness, CA based on 116 field-measured plots. Forest types were derived from combined CALVEG forest classes (see text for details). Plots were taken in summer of 2015

composites to limit the effects of cloud cover and atmospheric scattering. Tasseled-cap wetness (TCW) was calculated for each annual composited Landsat image using the formula defined by Crist and Cicone (1984). TCW was used for the analysis given its sensitivity to detecting changes in vegetation vigor, tree mortality, and canopy decline (Skakun et al. 2003; Meddens et al. 2013; Bell et al. 2018). To assess the relative decline across the entire time series, differenced ΔTCW images were calculated by differencing each sequential LandTrendr image in the image stack. The proportion of canopy decline within each year was then calculated by dividing the number of declined pixels in that year by the total number of pixels.

In order to characterize remotely-sensed canopy decline in terms of tree mortality, we compared a differenced TCW image between 2011 and 2016, representing a major drought period in California, with recent tree mortality from field measured data. Recent mortality included only snags that were considered a canopy dominant prior to mortality and had a decay class of one (presence of dead needles, branches and bark still intact). Field plots were classified into three bins based on the presence of recently dead snags: no snags (no decline), one to two snags (low decline), and more than three snags (high decline). Given that we were mainly concerned with the accuracy of our canopy decline maps, we chose not to limit our comparison to plots within the four CALVEG forest types. Plots with basal area < 1 m^2 were removed from the analysis, for a total of 140 plots. The differenced 2011–2016 image was resampled to 90 m to account for GPS inaccuracy in field plot locations. Decline thresholds were determined by iteratively assessing commission and omission errors using different thresholds, ultimately using thresholds that produced the lowest error values (Appendix A). Our goal was not necessarily a formal validation, but a coarse characterization of canopy decline and recent tree mortality.

Climate

Coarse-scale climate data was gathered from the Parameter-elevation Regression on Independent Slopes Model (PRISM, Daly et al. 2002) on a 2 km grid. PRISM interpolates climate data from a combination of instrumental records and topographic characteristics such as slope, aspect, elevation, and rain

shadows. Since four PRISM cells overlapped the study area, the average was taken of the two cells that contained the majority of the study area. Climate variables were generated for each year in the time series and included: maximum growing season temperature (Jun–Aug), minimum winter temperature (Dec–Feb), total water year precipitation (Oct–Sept), and minimum and maximum growing season vapor pressure deficit. Vapor pressure deficit is used as a measure of drought severity (Seager et al. 2015; Restaino et al. 2016) and represents the difference between the amount of moisture in the air and how much moisture can be held in the air once saturated. Most climate variables were obtained for the growing season (Jun–Aug) because it represents the highest vegetation vigor of any given year and coincides with the Landsat image acquisition dates. Minimum winter temperature was chosen as it is known to affect the reproduction of some bark beetle species (Bentz et al. 2010). Pearson product-moment correlation coefficients were generated between the composited TCW Landsat images and each climate variable for each year in the time series. All analyses were performed in R version 3.3.3 (R Core Development Team 2017).

Topographic and stand structure analysis

We derived three topographic metrics from a 30 m digital elevation model. Topographic variables included elevation, topographic position index (TPI, Jenness 2006), head load index (HLI, McCune and Keon 2002) and stand structure. TPI is a measure of slope position on a landscape, with lower values indicating sheltered valleys or ravines and higher values indicating more exposed ridges and hilltops. After multiple iterations with neighborhoods of different sizes, we decided that a 500 m circular neighborhood was best suited to characterize the topographic complexity of the landscape. HLI is a proxy for solar radiation in a given area and is based on aspect, slope, and coordinate position. Pixels were classified into one of four stand size classes using the CALVEG dataset: saplings (2.5 to 12.5 cm quadratic mean diameter [QMD]), small (12.7 to 25.1 cm QMD), medium (25.4 to 50.6 cm QMD), and large (50.8+ cm QMD). Continuous variables were classified into separate bins: elevation was divided into $<$ 1800 m, 1800–2000 m, 2000–2200 m, and > 2200 m; TPI was classified into valleys (< -140), lower

slopes (− 141 to 70), flat areas (− 69 to 0), middle slopes (1 to 70), upper slopes (71 to 141), and ridges (> 141); and HLI was classified into low (0 to 0.6), moderate (0.6 to 0.71), high (0.71 to 0.85), and very high (> 0.85), with low values representing cool northeastern slopes and high values representing hot southwestern slopes.

We started with a random sample of 5000 pixels from the canopy decline map between 2011 and 2016. We then used the correlog function from the ncf package in R (R Core Development Team 2017) to check for spatial autocorrelation in the data set. Results indicated spatial autocorrelation between pixels closer than 200 meters, leading us to reduce our sample to pixels that were at least 200 meters apart, for a total sample size of 619 pixels. We compared the magnitude of canopy decline among topographic settings using analysis of variance with the aov function in R (R Core Development Team 2017). We used the TukeyHSD function to test for pairwise differences between the different topographic settings. The assumption of equal variance was not met for TPI, so we used the kruskal.test function to perform a Kruskal–Wallis test as a non-parametric alternative to test for differences among topographic settings.

We used Fragstats (McGarigal and Marks 1995; McGarigal et al. 2012) to examine the size class distribution of patches of low and high canopy decline during the drought (2011 and 2016). Patch sizes were delineated using a 4-neighbor rule. This is a conservative estimate of patch size that delineates patches only among adjacent edges (i.e. cells with corners that touch are not considered part of a continuous patch).

Results

Field data

A total of 3446 canopy trees were measured across 116 plots (Fig. 1). The most abundant species sampled was white fir, followed by Shasta red fir and mountain hemlock. Across all taxa, the proportion of dead individuals was 17% (9.2% recently dead). Mortality varied by species, with the highest proportions of mortality occurring in subalpine fir (*Abies lasiocarpa*) at 35.3% (19.1% recently dead), Shasta red fir 28.6% (12.8% recent), and lodgepole pine at 22% (18.8%

recent). The total proportion of all species designated as unhealthy was 7.2%, with the highest proportions occurring in subalpine fir (19.1%) and Shasta red fir (16.2%). Engelmann spruce (*Picea engelmannii*), Brewer spruce (*Picea breweriana*), and Douglas-fir had the lowest proportions of mortality (7.8%, 9.5%, and 10.7% respectively), and lodgepole pine, ponderosa pine, and white fir had the lowest proportions of unhealthy trees (0.8%, 1.6%, and 2.2%).

Patterns of forest decline

We decided on decline thresholds at a 25-unit change (low decline) and an 83-unit change (high decline), representing the highest classification accuracy across all classes. Overall classification accuracy was 57.8%, but varied among decline classes and was highest for pixels classified as undisturbed and lowest for pixels classified as low decline (Appendix A in Supplementary Materials). Although classification was relatively poor at the pixel scale for the disturbed pixels (both low and high), commission and omission errors were fairly balanced and the proportion of area classified at different levels of canopy decline were consistent between the remotely sensed data and field measurements (Appendix B in Supplementary materials). Thus, we feel confident that our estimates of disturbed area across the study area are relatively robust despite the overall lack of high pixel scale classification accuracy.

The proportion of the study area that experienced canopy decline varied considerably throughout the time series (Fig. 3). The greatest proportions occurred in 2013 with 8.9% of the area experiencing decline, followed by 2014 with 6.8%. Of that area, 32.7% showed high levels of canopy decline in 2013, followed by 10.3% in 2014. Prior to 2013, all years experienced between 1% and 5% decline, with an average decline of 2.5%. A moderate pulse of canopy decline occurred between the years of 2000–2003, ranging from 3.9% to 4.5%. All forest types generally matched what was observed for the overall study area, with the highest levels of mortality being found in the last 4 years of the time series (Fig. 4). The highest proportion of decline occurred in the subalpine conifer forest type, with 12.4% of the area experiencing decline in 2013 and 9.5% in 2016. Red fir had the second highest proportions at 8.8% and 6.7% among the same years. Both mixed conifer and white fir forest
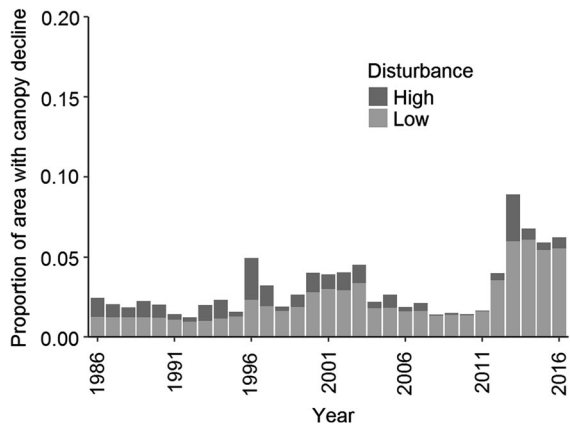
Fig. 3 Proportion of area experiencing canopy decline for each year of the LandTrendr time series for combined forest types. Low decline values were based on a 25-unit or greater decrease in tasseled cap wetness (TCW) between each year, while high decline was based on an 83-unit decrease

types had generally lower levels of decline in the last 4 years of the time series relative to other forest types (5.7–6% and 3–4% respectively). On average, 3.1% of the study area experienced decline across the entire time period. Of that, 24.5% was classified as high levels of decline.

Several moderately-sized patches of disturbance occurred across the study area, including one on the central-western side of the wilderness (∼ 200 ha) and another towards the south (∼ 130 ha, Fig. 5). Size-class distribution of patches of forest decline indicate a large number of patches > 1 ha across the landscape with relatively few larger than 25 ha (Fig. 6). Most areas with high decline occurred in patches smaller than 1 ha, with no patches larger than 10 ha.

Climate analysis

Significant correlations were found between some of our modelled climate variables and the estimated proportion of forest decline (Table 2). Maximum summer temperature and minimum vapor pressure deficit were positively correlated with canopy decline in all but the white fir forest type. Precipitation had the weakest correlation coefficients with little to no change across forest types, followed by minimum winter temperature which also had weak correlations for all forest types.
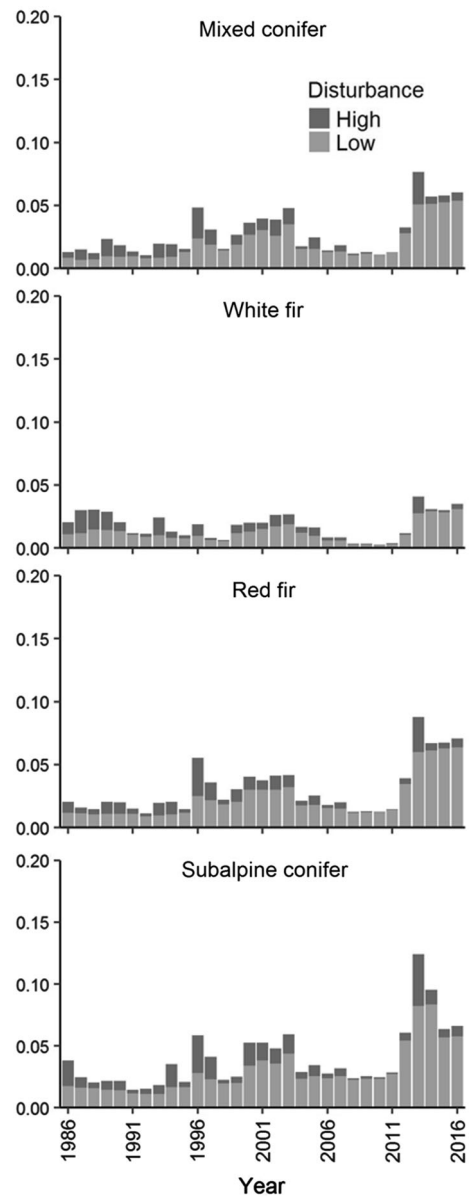
Fig. 4 Proportion of area disturbed for each year of the LandTrendr time series for each forest type. Low decline values were based on a 25-unit or greater decrease in tasseled cap wetness (TCW) between each year, while high decline was based on an 83-unit decrease. Note the elevated levels of disturbance in the red fir and subalpine conifer forest types

Topographic and stand structure analysis

We observed several differences in the magnitude of canopy decline values among stand structural classes (p < 0.001, F = 10.43). Stands with large QMD (representing old-growth characteristics) showed over
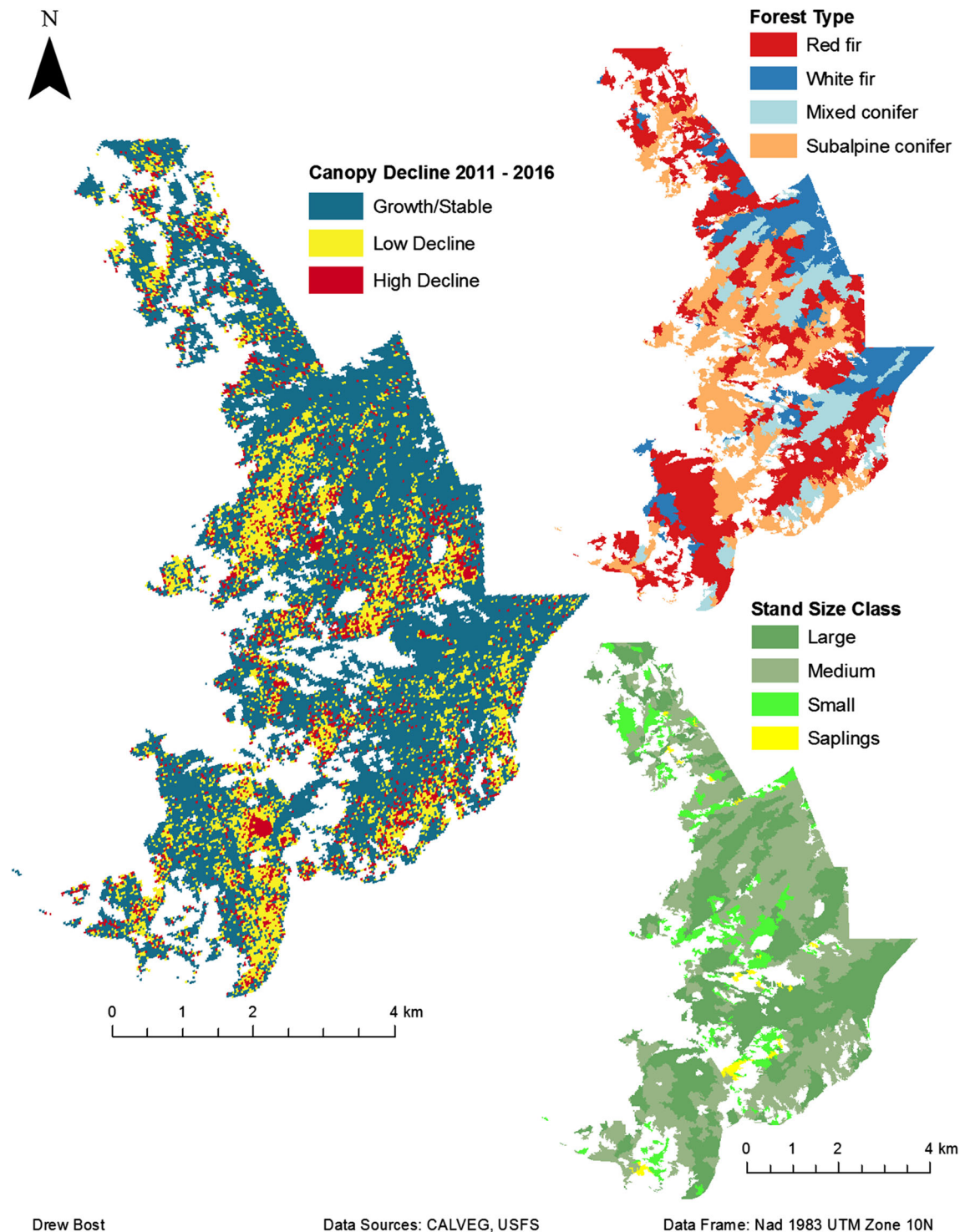
Fig. 5 Map of the Russian Wilderness, CA depicting the change in canopy decline between 2011 and 2016. Upper-right map depicts dominant forest types while lower-right map depicts forest stand size classes. Gaps indicate non-forested areas

Fig. 6 Size-class distributions of patches of low and high canopy decline between 2011 and 2016 in the Russian Wilderness, CA
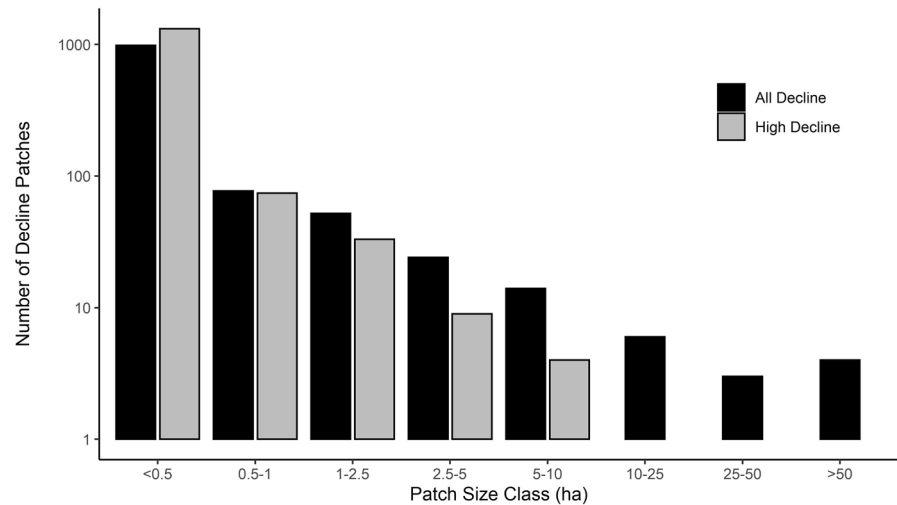
Table 2 Pearson product-moment correlation coefficients describing the relationship between climate variables and the proportion of area experiencing decline within each forest type

Climate variable	White fir	Mixed conifer	Subalpine conifer	Red fir	All
Minimum winter temperature	− 0.08	0.23	0.24	0.24	0.22
Maximum summer temperature	0.2	0.41**	0.45***	0.41**	0.43**
Minimum vapor pressure deficit	0.19	0.50***	0.46***	0.48***	0.47***
Maximum vapor pressure deficit	0.14	0.36*	0.33*	0.36*	0.35*
Total water year precipitation	− 0.21	− 0.10	− 0.04	− 0.06	− 0.08

Significant correlations are indicated by ***$p \leq 0.01$, **$p \leq 0.05$, $p < 0.1$*. All analyses were performed in R version 3.3.3

40% of pixels experiencing canopy decline, with little to no decline in all other stand structure classes.

We observed differences in the magnitude of decline among topographic settings with elevation ($p < 0.005$, F-value = 4.5) and HLI ($p = 0.009$, F = 3.88) but not TPI ($p = 0.29$, Chi square = 6.14) (Fig. 7). Significant pairwise differences ($p < 0.05$) were found between the two lowest and the two highest elevation bins. Nearly 50% of pixels in the upper elevation bin (2000–2200 m) experienced decline while relatively little decline was observed in elevations below 2000 m. Significant pairwise differences ($p < 0.05$) were found between the two lowest and two highest HLI classes. Roughly 40% of pixels that had a very high HLI (> 0.85) experienced canopy decline, compared to 0–5% in areas with low to high HLI (0–0.84). While there were no significant differences between TPI classes, roughly 90% of pixels that experienced canopy decline were in the

three highest classes (middle/upper slopes and ridges), compared to only 10% of valleys, flat areas, and lower slopes.

Discussion

This study provides a unique perspective on recent and pronounced increases in forest decline in one of North America's most diverse forested landscapes. Our analysis showed that levels of canopy decline were nearly three times greater in the last 4 years of the time series (2013–2016) than in the previous 26 years. However, canopy decline was not uniformly distributed across the landscape, and differed among topographic settings and stand structural conditions. The highest levels of canopy decline were found at mid to high elevations in dense red fir and subalpine conifer forests with old-growth forest attributes (i.e.,
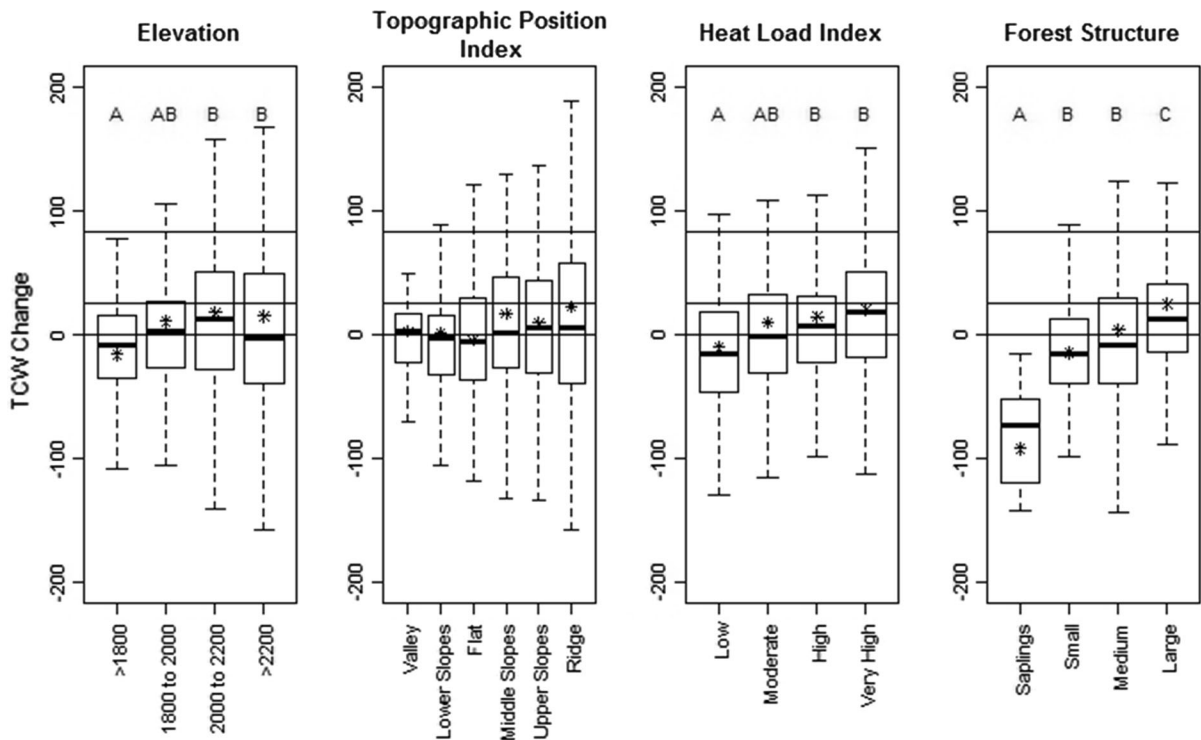
Fig. 7 Boxplots showing the relationship between TCW change and topographic and forest structure variables. TCW change values were taken from a differenced 2011–2016 LandTrendr image

large-diameter trees), suggesting that these forests may be particularly vulnerable to future mortality and decline events. This study supports the growing body of literature showing increases in tree mortality and forest decline (Allen et al. 2015) and demonstrates the vulnerability of high elevation old-growth forests to increasing temperature and decreased moisture availability.

In contrast to many remote sensing studies that document extremely large outbreaks of biotic disturbances in more homogenous forest types (i.e. mountain pine beetle in Rocky Mountain lodgepole pine forests, Meddens et al. 2012; Hicke et al. 2015), examining a much smaller and more diverse landscape enabled a greater focus on more nuanced effects of heterogeneity in stand structure, topography, and forest type. Our findings indicate that even under an extreme 5-year drought, canopy decline may be characterized by a few dominant canopy trees per pixel experiencing morality in occasional large patches (> 200 ha) embedded in a relatively fine-grained mosaic. The distribution of pixels that experienced high levels of decline across the last 4 years of

the time series was characterized predominantly by small (< 0.1 ha) patches, while total decline was dominated by several large patches that made up almost half of the total decline area (Fig. 6). The biggest patches of decline occur predominantly within large, homogenous patches of red fir and subalpine conifer forest types dominated by dense, old-growth forests (Fig. 5).

Our relatively low classification accuracy when comparing field-measured mortality to our ΔTCW values suggests that characterizing fine-grained patterns of subtle spectral changes in terms of mortality is challenging compared to higher levels of mortality observed in other studies with more homogenous landscapes and forest types (Appendix A in Supplementary Materials). A formal validation technique could help improve our remote sensing results and allow us to more accurately attribute changes in spectral values to tree mortality. This is especially true in more biologically diverse forest stands, where errors of omission are likely much higher due to the mixing of spectral signatures between live and dead trees. Validation may also help distinguish lower

levels of mortality that otherwise could not be detected from remote sensing data alone.

Our remote sensing and field data analysis reveals that most canopy decline in this study area is related to Shasta red fir mortality, both within Shasta red fir-dominated forests and in mixed forest types (Fig. 2). These findings are also supported by the fact that almost 50% of pixels within the elevation range of red fir experienced canopy decline (Fig. 7). DeSiervo et al. (2018) found that most Shasta red fir mortality was related to biotic agents including dwarf mistletoe and fir engraver beetle. Our findings are also consistent with a recent field-based study on red fir mortality in California. Mortenson et al. (2015) examined rates of red fir mortality based on re-measured trees in Forest Inventory and Analysis (FIA) plots across California (2000–2010) and found an annual mortality rate of 1.8%, generally coinciding with the elevated decline we observe over that same time period (Fig. 3). However, recent decline levels during a drought between 2011 and 2016 are nearly three times greater than the decline we observed from 2000 to 2010. The plot data also showed an unexpectedly high proportion of subalpine fir mortality (35%). Including the Russian Wilderness, subalpine fir is found in only eight locations in California which constitute the southern extent of this species range (Kauffmann 2012), but little is known regarding the status and trends of this species at other sites. Such rapid acceleration of forest decline in high elevation forests may pose a serious threat to forest biodiversity in this region, especially given projected increases in growing season temperatures (Reilly et al. 2018).

Fire suppression may be partially responsible for some of the recent conifer mortality occurring in the study area, particularly in the lower elevation mixed conifer and white fir forests. Prior to active fire exclusion, forests in the Klamath Mountains region were characterized by a low to mixed-severity fire regime, characterized by high frequency of low to moderate severity fire effects in mixed conifer forests (Skinner et al. 2006; Safford et al. 2011). Active suppression of fires in this region has led to fuel accumulation and increases in stand density (McKelvey et al. 1996; Gruell 2001; DiMario et al. 2018). Increased stand density from fire suppression has been shown to cause mortality through higher competition among trees (Dolph et al. 1995; Guarín and Taylor 2005; Ritchie et al. 2008; Maloney et al. 2011; Millar

et al. 2012). These denser stands may also facilitate the spread of pests and pathogens in landscapes dominated by large, contiguous patches of old-growth forest as observed in our study landscape. Although fire return intervals were longer in higher elevation forests types in this region, it is also possible that fire exclusion may be associated with some of the high levels of decline and mortality in red fir.

The greatest levels of canopy decline were observed in stands with larger trees (QMD > 50.8 cm), indicative of old-growth forest conditions in the region (Reilly and Spies 2016, Fig. 7). Over 40% of the area mapped as large trees experienced low to high decline with several large continuous patches of big trees corresponding with the largest patches of decline (Fig. 5). These findings are consistent with recent research highlighting the vulnerability of old-growth stands to climate change (van Mantgem et al. 2009) and biotic disturbance agents such as insects and pathogens (Reilly and Spies 2016). van Mantgem et al. (2009) documented a steady increase in background mortality rates of old-growth forests driven primarily by regional warming and water deficits from the mid-1950s to late 2000s. The elevated rates of decline we observed are consistent with those found by van Mantgem et al. (2009), particularly the moderate increase in mortality rates from 2000 to 2005 ranging from a 3% to 6% increase. While these background rates of mortality are consistent between the two studies, van Mantgem et al.'s (2009) study did not assess the extreme drought that began in California in 2011 where we observed elevated levels of canopy decline.

Differences in the distribution of declined pixels among topographic settings supports the role of topographic refugia from high temperatures during extreme drought. While there were no significant differences between TPI classes, ∼ 90% of pixels that experienced canopy decline during the drought period occurred on more exposed mid-slopes, upper slopes and ridges, whereas the more sheltered valleys and ravines experienced almost no canopy decline during the same time period (Fig. 7). We observed significant differences between the higher and lower HLI classes, with nearly half of the pixels in higher classes experiencing canopy decline. These results suggest that not all positions in the landscape experience drought or high temperatures the same. In contrast, Paz-Kagan et al. (2017) found an increased

probability of tree mortality on shallower slopes and at lower elevations in the southern Sierra Nevada Mountains of California where temperatures are likely much warmer. It is possible that the high topographic complexity in the Russian Wilderness creates more opportunity for refugia than other parts of California and potentially tempers the impacts of drought in this region. In addition to topographic shading and drainage of cooler air at night, old-growth vegetation has the potential to mitigate increases in temperature in topographically complex landscapes (Daly et al. 2010; Dobrowski 2011; Frey et al. 2016). Our results are ecologically significant given that identification of climate refugia has proven difficult and much of the conversation surrounding the issue has been largely descriptive (Keppel et al. 2012; Morelli et al. 2016). Given the relatively small landscape in this study, further analysis at a larger spatial extent could help assess the consistency of these results in other parts of the region.

With the exception of lower elevation white fir forests, maximum summer temperature and minimum vapor pressure deficit were the primary climatic drivers of forest decline over the 30-year study period. Although the strength of the correlations varied among forest types, these results are consistent with other studies that found temperature as a primary driver of tree mortality in other regions of the western US (Williams et al. 2013). Interestingly, of the two VPD variables used in the analysis, only minimum VPD was significantly correlated with canopy decline, indicating that rather than extreme climate events driving canopy decline, more subtle shifts in baseline climatic conditions may be greater contributors to an overall decrease in forest health. Precipitation showed little relationship with forest decline, a result that was consistent with the DeSiervo et al. (2018) analysis. While much of California has experienced record-setting droughts between 2011 and 2016, Rapacciuolo et al. (2014) demonstrated that precipitation patterns across the region are geographically variable, with some areas of the Klamath showing increases in precipitation while others showing little to no change. Recent research has also highlighted this potential decrease in influence of precipitation on forest mortality in California (Wahl et al. 2019). Given the role of topographic complexity in landscape-scale variation in decline, a more complex analysis with downscaled climate data may help elucidate fine-scale

interactions as well as landscape-level trends regarding the interaction between climate and canopy decline in this region.

Conclusions

This study provides valuable insight into a recent mortality event in a highly diverse conifer forest of northern California. Our findings highlight trends of canopy decline in high elevations forests, specifically Shasta red fir and subalpine conifer forest types, and highlights the need for more research and monitoring to be conducted regarding the casual agents driving this mortality. Our study exemplifies the difficulties in predicting and classifying low levels of tree mortality in highly heterogeneous ecosystems, but by leveraging complimentary data sources (i.e. field observations and remote sensing), we are able to provide more ecological context than by either source alone. Given projections of increases in temperature into the future, we expect the observed trends to continue. However, a more comprehensive study of the interactions between climate and canopy decline may elucidate climatic drivers of decline and help to identify the greatest vulnerabilities to future climate change. This work contributes to the growing body of evidence indicating increased levels of mortality among forests of western North America, and the roles that climate, stand structure, and topography play in driving and shaping this mortality across a diverse and heterogeneous landscape.

References

Allen CD, Macalady AK, Chenchouni H, Bachelet D, McDowell N, Vennetier M, Kitzberger T, Rigling A, Breshears DD, Hogg EH, Gonzalez P, Fensham R, Zhangm Z, Castro J, Demidova N, Lim JH, Allard G, Running SW, Semerci A, Cobb N (2010) A global overview of drought

and heat-induced tree mortality reveals emerging climate change risks for forests. For Ecol Manag 259(4):660–684

Allen CD, Breshears DD, McDowell NG (2015) On underestimation of global vulnerability to tree mortality and forest die-off from hotter drought in the Anthropocene. Ecosphere 6(8):1–55

Anderegg WRL, Kane JM, Anderegg LDL (2012) Consequences of widespread tree mortality triggered by drought and temperature stress. Nat Clim Change 3(1):30–36

Battles JJ, Robards T, Das A, Waring K, Gilless JK, Biging G, Schurr F (2008) Climate change impacts on forest growth and tree mortality: a data-driven modeling study in the mixed-conifer forest of the Sierra Nevada, California. Clim Change 87(S1):193–213

Bekker MF, Taylor AH (2001) Gradient analysis of fire regimes in montane forests of the southern Cascade range, Thousand Lakes Wilderness, California, USA. Plant Ecol 155:15–28

Bekker MF, Taylor AH (2010) Fire disturbance, forest structure, and stand dynamics in montane forests of the southern Cascades, Thousand Lakes Wilderness, California, USA. Ecoscience 17:59–72

Bell DM, Cohen WB, Reilly M, Yang Z (2018) Visual interpretation and time series modeling of Landsat imagery highlight drought's role in forest canopy declines. Ecosphere 9(6):e02195

Bentz BJ, Régnière J, Fettig CJ, Hansen EM, Hayes JL, Hicke JA, Kelsey RG, Negrón JF, Seybold SJ (2010) Climate change and bark beetles of the western United States and Canada: direct and indirect effects. Bioscience 60(8):602–613

Biederman JA, Brooks PD, Harpold AA, Gochis DJ, Gutmann E, Reed DE, Pendall E, Ewers BE (2014) Multiscale observations of snow accumulation and peak snowpack following widespread, insect-induced lodgepole pine mortality. Ecohydrology 7(1):150–162

Cline SP, Berg AB, Wight HM (1980) Snag characteristics and dynamics in Douglas-fir forests, Western Oregon. J Wildl Manag 40(4):773–786

Cohen WB, Yang Z, Kennedy R (2010) Detecting trends in forest disturbance and recovery using yearly Landsat time series: 2 TimeSync—Tools for calibration and validation. Remote Sens Environ 114(12):2911–2924

Cohen WB, Yang Z, Stehman SV, Schroeder TA, Bell DM, Masek JG, Huang C, Meigs GW (2016) Forest disturbance across the conterminous United States from 1985–2012: the emerging dominance of forest decline. For Ecol Manag 360:242–252

Coleman RG, Kruckeberg AR (1999) Geology and plant life of the Klamath-Siskiyou Mountain region. Nat Areas J 19(4):320–340

Copeland SM, Harrison SP, Latimer AM, Damschen EI, Eskelinen AM, Fernandez-Going B, Spasojevic MJ, Anacker BL, Thorne JH (2016) Ecological effects of extreme drought on Californian herbaceous plant communities. Ecol Monogr 86(3):295–311

Crist EP, Cicone RC (1984) A physically-based transformation of thematic mapper data—the TM tasseled cap IEEE. Trans Geosci Remote Sens GE 22(3):256–263

Daly C, Gibson WP, Taylor GH, Johnson GL, Pasteris P (2002) A knowledge-based approach to the statistical mapping of climate. Clim Res 22(2):99–113

Daly C, Conklin DR, Unsworth MH (2010) Local atmospheric decoupling in complex topography alters climate change impacts. Int J Climatol 30(12):1857–1864

DeSiervo MH, Jules ES, Bost DS, Stigter DLE, Butz RJ (2018) Patterns and drivers of recent tree mortality in diverse conifer forests of the Klamath Mountains, California. For Sci 64(4):371–382

DiMario AA, Kane JM, Jules ES (2018) Characterizing forest floor fuels surrounding large sugar pine (*Pinus lambertiana*) in the Klamath Mountains, California. Northwest Sci 92(3):181–190

Dobrowski SZ (2011) A climatic basis for microrefugia: the influence of terrain on climate. Glob Change Biol 17(2):1022–1035

Dolph KL, Mori SR, Oliver WM (1995) Long-term responses of old-growth stands to varying levels of partial cutting in the eastside pine type. West J Appl For 10:101–108

Frey SJK, Hadley AS, Johnson SL, Schulze M, Jones JA, Betts MG (2016) Spatial models reveal the microclimatic buffering capacity of old-growth forests. Sci Adv 2(4):e1501392

Goodwin NR, Coops NC, Wulder MA, Gillanders S, Schroeder TA, Nelson T (2008) Estimation of insect infestation dynamics using a temporal sequence of Landsat data. Remote Sens Environ 112(9):3680–3689

Gruell GE (2001) Fire in Sierra Nevada forests: a photographic interpretation of ecological change since 1849. Mountain Press, Missoula

Guarín A, Taylor AH (2005) Drought triggered tree mortality in mixed conifer forests in Yosemite National Park, California, USA. For Ecol Manag 218(1–3):229–244

Hart SJ, Veblen TT, Schneider D, Molotch NP (2017) Summer and winter drought drive the initiation and spread of spruce beetle outbreak. Ecology 98(10):2698–2707

Hicke JA, Meddens AJ, Kolden CA (2015) Recent tree mortality in the western United States from bark beetles and forest fires. For Sci 62(2):141–153

Jenness J (2006) Topographic position index extension for ArcView 3x, v 13a. Jenness Enterprises. http://www.jennessent.com/downloads/tpi_documentation_online.pdf. Accessed 27 Dec 2018

Kauffmann ME (2012) Conifer country: a natural history and hiking guide to 35 conifers of the Klamath Mountain region. Backcountry Press, Kneeland

Keeler-Wolf T (1984) Vegetation map of the upper Sugar Creek drainage, Siskiyou County. Unpublished report on file. Pacific Southwest Research Station, Albany

Kennedy RE, Townsend PA, Gross JE, Cohen WB, Bolstad P, Wang YQ, Adams P (2009) Remote sensing change detection tools for natural resource managers: understanding concepts and tradeoffs in the design of landscape monitoring projects. Remote Sens Environ 113(7):1382–1396

Kennedy RE, Yang Z, Cohen WB (2010) Detecting trends in forest disturbance and recovery using yearly Landsat time series: 1 LandTrendr—temporal segmentation algorithms. Remote Sens Environ 114(12):2897–2910

Kennedy RE, Yang Z, Cohen WB, Pfaff E, Braaten J, Nelson P (2012) Spatial and temporal patterns of forest disturbance and regrowth within the area of the Northwest Forest Plan. Remote Sens Environ 122:117–133

Keppel G, Van Niel KP, Wardell-Johnson GW, Yates CJ, Byrne M, Mucina L, Schut AGT, Hopper SD, Franklin SE (2012) Refugia: identifying and understanding safe havens for biodiversity under climate change. Glob Ecol Biogeogr 21(4):393–404

Klos RJ, Wang GG, Bauerle WL, Rieck JR (2009) Drought impact on forest growth and mortality in the southeast USA: an analysis using Forest Health and Monitoring data. Ecol Appl 19(3):699–708

Maloney PE, Vogler DR, Eckert AJ, Jensen CE, Neale DB (2011) Population biology of sugar pine (*Pinus lambertiana* Dougl) with reference to historical disturbances in the Lake Tahoe Basin: implications for restoration. For Ecol Manage 262(5):770–779

Manion PD (1991) Tree disease concepts, 2nd edn. Prentice-Hall, Englewood Cliffs

McCune B, Keon D (2002) Equations for potential annual direct incident radiation and heat load. J Veg Sci 13(4):603–606

McGarigal K, Marks BJ (1995) FRAGSTATS: spatial pattern analysis program for quantifying landscape structure. Gen Tech Rep PNW-GTR-351. US. Department of Agriculture, Forest Service, Pacific Northwest Research Station, Portland, OR, vol 122, p 351

McGarigal K, Cushman SA, Ene E (2012) FRAGSTATS v4: spatial pattern analysis program for categorical and continuous maps computer software program. Produced by the authors at the University of Massachusetts, Amherst

McKelvey KS, Skinner CN, Chang C, Erman DC, Husari SJ, Parsons DJ, van Wagtendonk JW, Weatherspoon PC (1996) An overview of fire in the Sierra Nevada. In: Sierra Nevada Ecosystem Project, final report to congress, vol II. Assessments and Scientific Basis for Management Options Davis, CA, University of California, Centers for Water and Wildland Resources Report No 37, pp 1033–1040

Meddens AJH, Hicke JA, Ferguson CA (2012) Spatiotemporal patterns of observed bark beetle-caused tree mortality in British Columbia and the western United States. Ecol Appl 22(7):1876–1891

Meddens AJH, Hicke JA, Vierling LA, Hudak AT (2013) Evaluating methods to detect bark beetle-caused tree mortality using single-date and multi-date Landsat imagery. Remote Sens Environ 132:49–58

Millar CI, Westfall RD, Delany DL, Bokach MJ, Flint AL, Flint LE (2012) Forest mortality in high-elevation whitebark pine (*Pinus albicaulis*) forests of eastern California, USA; influence of environmental context, bark beetles, climatic water deficit, and warming. Can J For Res 42(4):749–765

Miller JD, Safford HD, Crimmins M, Thode AE (2009) Quantitative evidence for increasing forest fire severity in the Sierra Nevada and Southern Cascade Mountains, California and Nevada, USA. Ecosystems 12(1):16–32

Morawitz DF, Blewett TM, Cohen A, Alberti M (2006) Using NDVI to assess vegetative land cover change in central Puget Sound. Environ Monit Assess 114(1–3):85–106

Morelli TL, Daly C, Dobrowski SZ, Dulen DM, Ebersole JL, Jackson ST, Lundquist JD, Millar CI, Maher SP, Monahan WB, Nydick KR, Redmond KT, Sawyer SC, Stock S,
Beissinger SR (2016) Managing climate change refugia for climate adaptation. PLoS ONE 11(8):e0159909

Mortenson L, Gray AN, Shaw DC (2015) A forest health inventory assessment of red fir (*Abies magnifica*) in upper montane California. Ecoscience 22(1):47–58

Odion DC, Frost EJ, Strittholt JR, Jiang H, Dellasala DA, Moritz MA (2004) Patterns of fire severity and forest conditions in the western Klamath Mountains, California. Conserv Biol 18(4):927–936

Parker I, Matyas W (1979) CALVEG: a classification of Californian vegetation. US Department of Agriculture, Forest Service, Pacific Southwest Region Station, Albany

Paz-Kagan T, Brodrick PG, Vaughn NR, Das AJ, Stephenson NL, Nydick KR, Asner GP (2017) What mediates tree mortality during drought in the southern Sierra Nevada? Ecol Appl 27:2443–2457

Potter C (2016) Thirty years of vegetation change in the coastal Santa Cruz Mountains of Northern California detected using landsat satellite image analysis. J Coast Conserv 20(1):51–59

R Core Development Team (2017) R: a language and environment for statistical computing. R Foundation for Statistical Computing, Vienna

Rapacciuolo G, Maher SP, Schneider AC, Hammond TT, Jabis MD, Walsh RE, Iknayan KJ, Walden GK, Oldfather MF, Ackerly DD, Beissinger SR (2014) Beyond a warming fingerprint: individualistic biogeographic responses to heterogeneous climate change in California. Glob Change Biol 20(9):2841–2855

Reilly MJ, Spies TA (2016) Disturbance, tree mortality, and implications of regional forest change in the Pacific Northwest. For Ecol Manag 374:102–110

Reilly MJ, Spies TA, Littell J, Butz R, Kim J (2018) Vulnerability of vegetation to climate change and disturbance in the Northwest Forest Plan area. In: Synthesis of science to inform land management within the Northwest Forest Plan Area. USFS PNW GTR-966 vol 1

Restaino CM, Peterson DL, Littell J (2016) Increased water deficit decreases Douglas fir growth throughout western US forests. Proc Natl Acad Sci 113(34):9557–9562

Ritchie MW, Wing BM, Hamilton TA (2008) Stability of the large tree component in treated and untreated late-seral interior ponderosa pine stands. Can J For Res 38:919–923

Safford HD, Van de Water KM (2014) Using fire return interval departure (FRID) analysis to map spatial and temporal changes in fire frequency on national forest lands in California. US Department of Agriculture, Forest Service, Pacific Southwest Research Station, vol 59, p 266

Safford HD, van de Water K, Schmidt D (2011) California fire return interval departure (FRID) map metadata: description of purpose, data sources, database fields, and their calculations. USDA Forest Service, Pacific Southwest Region, Vallejo

Sawyer JO (2007) Why are the Klamath Mountains and adjacent North Coast floristically diverse? Fremontia 35(3):3–11

Sawyer JO, Thornburgh DA (1971) Vegetation types on granodiorite in the Klamath Mountains, California. Report to the Pacific Southwest Forest and Range Experiment Station, Berkeley, California PSW COOP-AID agreement supplement #10 unpublished report on file, Pacific Southwest Research Station, Albany, California

Sawyer JO, Thornburgh DA (1974) Subalpine and montane forests on granodiorite in the central Klamath Mountains of California. Unpublished report to Pacific Southwest Forest and Range Exp. Sta., Berkeley, California

Seager R, Hooks A, Williams AP, Cook B, Nakamura J, Henderson N (2015) Climatology, variability, and trends in the US vapor pressure deficit, an important fire-related meteorological quantity. J Appl Meteorol Climatol 54(6):1121–1141

Skakun RS, Wulder MA, Franklin SE (2003) Sensitivity of the thematic mapper enhanced wetness difference index to detect mountain pine beetle red-attack damage. Remote Sens Environ 86(4):433–443

Skinner CN (2003) Fire history of upper montane and subalpine lake basins in the Klamath Mountains of northern California. In: Proceedings of fire conference 2000: the first national congress on fire ecology, prevention and management, Misc. Pub. 13 Tall Timbers Research Station, Tallahassee, FL, pp 145–151

Skinner CN, Taylor AH, Agee JK (2006) Klamath mountain bioregion. In: Sugihara NG, van Wagtendonk JW, Shaffer KE, Fites-Kaufman J, Thode AE (eds) Fire in California's ecosystems. The University of California Press, Berkeley, pp 170–194

Stebbins GL, Major J (1965) Endemism and speciation in the California Flora. Ecol Monogr 35(1):1–35

Taylor AH (1993) Fire history and structure of red fir (*Abies magnifica*) forests, Swain Mountain Experimental Forest, Cascade Range, northeastern California. Can J For Res 23(8):1672–1678

Taylor AH (2000) Fire regimes and forest changes in mid and upper montane forests of the southern Cascades, Lassen Volcanic National Park, California, USA. J Biogeogr 27:87–104

Taylor AH, Halpern CB (1991) The structure and dynamics of *Abies magnifica* forests in the southern Cascades Range, USA. J Veg Sci 2:189–200

Taylor AH, Skinner CN (1998) Fire history and landscape dynamics in a late-successional reserve, Klamath Mountains, California, USA. For Ecol Manag 111(2–3):285–301

Taylor AH, Skinner CN (2003) Spatial patterns and controls on historical fire regimes and forest structure in the Klamath Mountains. Ecol Appl 13(3):704–719

van der Molen MK, Dolman AJ, Ciais P, Eglin T, Gobron N, Law BE, Meir P, Peters W, Phillips OL, Reichstein M, Chen T, Dekker SC, Doubková M, Friedl MA, Jung M, van den Hurk BJJM, de Jeu RAM, Kruijt B, Ohta T, Rebel KT, Plummer S, Seneviratne SI, Sitch S, Teuling AJ, van der Werf GR, Wang G (2011) Drought and ecosystem carbon cycling. Agric For Meteorol 151(7):765–773

Van Gunst KJ, Weisberg PJ, Yang J, Fan Y (2016) Do denser forests have greater risk of tree mortality: a remote sensing analysis of density-dependent forest mortality. For Ecol Manag 359:19–32

van Mantgem PJ, Stephenson NL (2007) Apparent climatically induced increase of tree mortality rates in a temperate forest. Ecol Lett 10(10):909–916

van Mantgem PJ, Stephenson NL, Byrne JC, Daniels LD, Franklin JF, Ful PZ (2009) Widespread increase of tree mortality rates in the western United States. Science 323(5913):521–524

Vogelmann JE, Tolk B, Zhu Z (2009) Monitoring forest changes in the southwestern United States using multitemporal Landsat data. Remote Sens Environ 113(8):1739–1748

Wahl ER, Zorita E, Trouet V, Taylor AH (2019) Jet stream dynamics, hydroclimate, and fire in California from 1600 CE to present. Proc Natl Acad Sci 116(12):5393–5398

Whittaker RH (1960) Vegetation of the Siskiyou mountains, Oregon and California. Ecol Monogr 30(3):279–338

Williams DW, Liebhold AM (2002) Climate change and the outbreak ranges of two North American bark beetles. Agric For Entomol 4(2):87–99

Williams AP, Allen CD, Macalady AK, Griffin D, Woodhouse C, Meko D, Swetnam T, Rauscher Seager R, Grissino-Mayer HD, Dean JS, Cook ER, Gangodagamage C, Cai M, McDowell NG (2013) Temperature as a potent driver of regional forest drought stress and tree mortality. Nat Clim Change 3(3):292–297

Wills RD, Stuart JD (1994) Fire history and stand development of a Douglas-fir/hardwood forest in northern California. Northwest Sci 68(3):205–212

Wulder MA, White JC, Coops NC, Butson CR (2008) Multi-temporal analysis of high spatial resolution imagery for disturbance monitoring. Remote Sens Environ 112(6):2729–2740